

Communication

Effect of Nickel Doping on the Cure Kinetics of Epoxy/Fe₃O₄ Nanocomposites

Maryam Jouyandeh ¹, Zohre Karami ¹, Seyed Mohammad Reza Paran ¹,
Amin Hamed Mashhadzadeh ¹ , Mohammad Reza Ganjali ^{1,2}, Babak Bagheri ³,
Payam Zarrintaj ⁴ , Sajjad Habibzadeh ⁵, Poornima Vijayan P. ⁶
and Mohammad Reza Saeb ^{1,*}

¹ Center of Excellence in Electrochemistry, School of Chemistry, College of Science, University of Tehran, Tehran 11155-4563, Iran; maryam.jouyande@gmail.com (M.J.); zohrekarami.2013@yahoo.com (Z.K.); smrparan@gmail.com (S.M.R.P.); amin.hamed.m@gmail.com (A.H.M.); ganjali@ut.ac.ir (M.R.G.)

² Biosensor Research Center, Endocrinology and Metabolism Molecular-Cellular Sciences Institute, Tehran University of Medical Sciences, Tehran 11155-4563, Iran

³ Department of Chemical and Biomolecular Engineering, Korea Advanced Institute of Science and Technology (KAIST), Daejeon 34141, Korea; babakbagheri@kaist.ac.kr

⁴ School of Chemical Engineering, Oklahoma State University, 420 Engineering North, Stillwater, OK 74078, USA; payam.zarrintaj@okstate.edu

⁵ Department of Chemical Engineering, Amirkabir University of Technology (Tehran Polytechnic), Tehran 1591639675, Iran; sajjad.habibzadeh@aut.ac.ir

⁶ Department of Chemistry, Sree Narayana College for Women (Affiliated to University of Kerala), Kollam, Kerala 691001, India; poornimavijayan2007@gmail.com

* Correspondence: mrsaeb2008@gmail.com; Tel.: +98-(912)-8264307

Received: 20 June 2020; Accepted: 28 July 2020; Published: 30 July 2020



Abstract: This short communication aims to evaluate the cure kinetics of epoxy/Ni_xFe_{3-x}O₄ nanocomposites. Differential scanning calorimetry (DSC) provided support for cure kinetics analysis based on the variation of activation energy ($E\alpha$) as a function of the extent of crosslinking reaction, α . The average values of $E\alpha$ calculated based on Kissinger and Friedman methods were 59.22 and 57.35 kJ/mol for the neat epoxy, 43.37 and 48.74 kJ/mol for the epoxy/Fe₃O₄, and eventually 50.48 and 49.19 kJ/mol for the epoxy/Ni_xFe_{3-x}O₄ nanocomposites. The partial replacement of Fe²⁺ ion sites in the Fe₃O₄ crystal lattice by the Ni²⁺ ions changed to some content the cure kinetic profile because of the fact that a lower level of energy was needed for curing by incorporation of Ni_xFe_{3-x}O₄ into the epoxy matrix. The rate of reaction calculated theoretically adequately fitted with experimental profiles obtained in DSC experiments.

Keywords: cure kinetics; magnetic nanoparticles; epoxy nanocomposites; coatings

1. Problem Description

Epoxy/iron oxide nanocomposites are used in the development of anticorrosion coatings. There are two main questions to be answered in the field of epoxy/iron oxide nanocomposites and nanocomposite coating: (i) which metal dopant together with a reactive molecule, respectively, present in the bulk and on the surface of nanoparticles can change the kinetics of epoxy cure reaction?; and (ii) does a small amount of iron oxide (below 0.2 wt % based on epoxy resin) affect the curing reaction of epoxy? Understanding the correlation between cure kinetics and the ultimate properties of epoxy composites gives useful insight into the performance of epoxy composites [1,2]. In the case of thermoset composites, complexities are involved in the interaction between the polymer chains and fillers [3,4]. Nevertheless, a few have talked about the effect of nanoparticles on the crosslinking of resins in

such systems as well as their thermal, mechanical and corrosion properties. The limited information on molecular-level events taking place in the epoxy nanocomposites makes it difficult to interpret their ultimate properties. A complete cure is commonly the result of the appropriate dispersion of nanoparticles in the viscous liquid-like resin, which itself determines the nanoparticle–epoxy interaction [5,6]. The addition of nanoparticles to the epoxy system can facilitate or perturb curing reactions depending on the shape, size, loading and the functionality of nanoparticles [7–9]. To precisely monitor the effect of nanoparticles on the ultimate properties, one may need to analyze the cure reaction of epoxy nanocomposites. Investigating the macro behavior of epoxy nanocomposites from a microstructure perspective enables researchers to optimize the preferred properties. Therefore, to have high-performance epoxy nanocomposites, one needs to understand the relationship between the microstructure and crosslinking reaction in the system. For example, the anticorrosion properties of epoxy nanocomposite coatings are dominated by the barrier mechanism. Therefore, the barrier inhibition and anticorrosion property of the epoxy system both depend on the completeness of the crosslinking of resin in the presence of nanoparticles [10]. Shi et al. [11] showed that the SiO₂ nanoparticles tend to bridge the interconnected matrix and cause a reduction in the total free volume. As a result, the crosslinking density of the epoxy system has been improved. Highly cured epoxy/SiO₂ nanocomposite increased the barrier performance and anticorrosion properties of coatings. In addition, it is reported that the cured epoxy/SiO₂ nanocomposite improves the stiffness of epoxy coatings by lowering the chain segmental motions. However, Fe₂O₃ nanoparticles could agglomerate during the curing of epoxy which later plays the role of stress concentrator forming microcracks that weaken the corrosion inhibition and Young's modulus of coatings. Madhup et al. [12] indicated that by the addition of 5 wt % of ammonium-modified clay nanoparticles to the epoxy matrix, the abrasion resistance of epoxy nanocomposite decreased as a consequence of the network being partially cured.

The use of the Cure Index (CI) helped the classification of the cure state of thermoset composites [13]. This gauge allows for a quick understanding of structure–property relationships in the thermoset composites [14–17]. However, it has been classically demonstrated that the molecular mechanism of crosslinking reactions could be more precisely explained by the cure kinetics studies [18]. The cure behavior and kinetics of epoxy-based nanocomposites containing different types of nanoparticles have been developed in this group by focusing on surface modification with different functional groups [19,20]. In a previous study, Fe₃O₄ nanoparticles have been electrochemically synthesized and the nickel doped Fe₃O₄ (Ni_xFe_{3-x}O₄) was produced [21]. The investigations suggested that crosslink density of the epoxy network cured with an amine curing agent was affected by the introduction of Fe₃O₄ and Ni-doped Fe₃O₄ to epoxy resin, as reflected in the changes in the values of the CI. The need for deepening the molecular interpretation of cure kinetics was the reason for this investigation. Herein, the effects of Fe₃O₄ and Ni-doped Fe₃O₄ on the cure kinetics of the epoxy/amine system were classically studied by isoconversional differential scanning calorimetry (DSC) analyses. The triplet of cure parameters (*n*, *m* and ln*A*) was monitored based on modeling with isoconversional methods.

2. Development and Characterization of Nanocomposite

2.1. Chemicals

Epoxy matrix (Epon-828, epoxide equivalent weight of 185–192 g/eq.) and curing agent (triethylenetetramine (TETA), hydrogen equivalent weight of 25 g/eq.) were supplied by Hexion, Beijing (China). The chemical structure of the epoxy resin and curing agent are shown in Figure 1.

2.2. Preparation of Epoxy Nanocomposites

First, 0.1 wt % of bare Fe₃O₄ and Ni-Fe₃O₄ were separately added to the epoxy resin to prepare EP/Fe₃O₄, EP/Ni-Fe₃O₄ nanocomposites, respectively. After the addition of nanoparticles to the mixture, it was sonicated for 5 min followed by further mixing with a mechanical mixer working at

2500 rpm for 20 min. Just before the DSC test, the stoichiometric amount of TETA was added to the epoxy resin (hardener/epoxy ratio was 13:100) and mixed homogeneously.

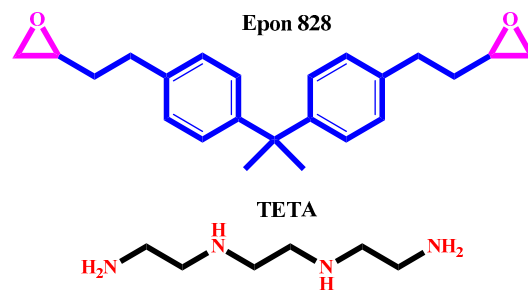


Figure 1. Chemical structure of Epon 828 and TETA.

2.3. Characterization of Epoxy Nanocomposites

The cure reaction of epoxy/amine system (the neat epoxy and the nanocomposites containing 0.1 wt % of bare Fe₃O₄ and Ni-Fe₃O₄) was investigated by DSC on Perkin Elmer DSC 4000. Dynamic DSC was performed at heating rates of 5, 10, 15 and 20 °C/min from 15 to 250 °C under nitrogen flow rate of 20 mL/min. Experiments at the rate of 10 °C/min were reciprocally performed through heating–cooling–heating cycle to record glass transition temperature (T_g).

3. Quantitative Cure Analysis

The cure kinetics of the systems was performed based on a recent protocol in terms of cure behavior and cure kinetics [18].

3.1. Cure Behavior Analysis

Figure 2 shows DSC thermograms of the neat epoxy and its nanocomposites containing 0.1 wt % of Fe₃O₄ and Ni-Fe₃O₄ at four different heating rates of 5, 10, 15 and 20 °C/min. The unimodal peak in the DSC curves confirmed the assumption that the kinetic reaction was a single step [22,23]. As expected, the peak temperature of DSC thermograms shifted towards higher values upon increasing the heating rate, which can be attributed to the higher kinetic energy per molecule in the system achieved at a higher heating rate [24,25].

The two main phenomena taking place during the crosslinking reaction of epoxy resin are gelation (liquid to rubber transition) and vitrification (liquid or rubber to glass transition). Gelation is an irreversible phenomenon that occurs at a certain degree of conversion (α_{gel}). By contrast, vitrification is a gradual and thermo-reversible phenomenon [27]. In addition, the curing process of epoxy with an amine curing agent occurs in several steps. The hydrogen group of primary amine reacts with an oxirane ring of epoxy resin to form secondary amines at an early stage of curing reaction. The crosslinking reaction of epoxy with the hydrogen of secondary amine occurs at a later stage of the curing process due to the less reactivity and accessibility to epoxide groups in a highly viscous system. Moreover, some hydroxyl groups form during the epoxide ring-opening by the primary and secondary amine. These OH groups with less reactivity compared to the hydrogen groups of primary and secondary amine can further catalyze the epoxide ring via etherification reaction at the final stages of curing at higher temperatures. The chemical schemes of the curing reaction of epoxy with amine are typically shown in Figure 3.

The amount of heat release caused by a crosslinking reaction in the thermosetting systems can be calculated by the extent of the reaction progress, α according to the Equation (1):

$$\alpha = \frac{\Delta H_T}{\Delta H_\infty}, \quad (1)$$

where ΔH_{∞} and ΔH_T are the total heat released during the cure reaction (from the onset temperature to the endset temperature) and the total heat release at a given temperature T , respectively. Figure 4 shows the variation pattern of α as a function of time of cure reaction of the neat epoxy, as well as EP/Fe₃O₄ and EP/Ni-Fe₃O₄ nanocomposites at different heating rates. The conversion profiles are sigmoidal in the form independent of the heating rate, which is characteristic of the autocatalytic mechanism of curing reaction [28]. Noticeably, the shape of conversion profiles remained unaffected by adding Fe₃O₄ and Ni-Fe₃O₄ nanoparticles, which is indicative of the dominance of autocatalytic reactions in the system.

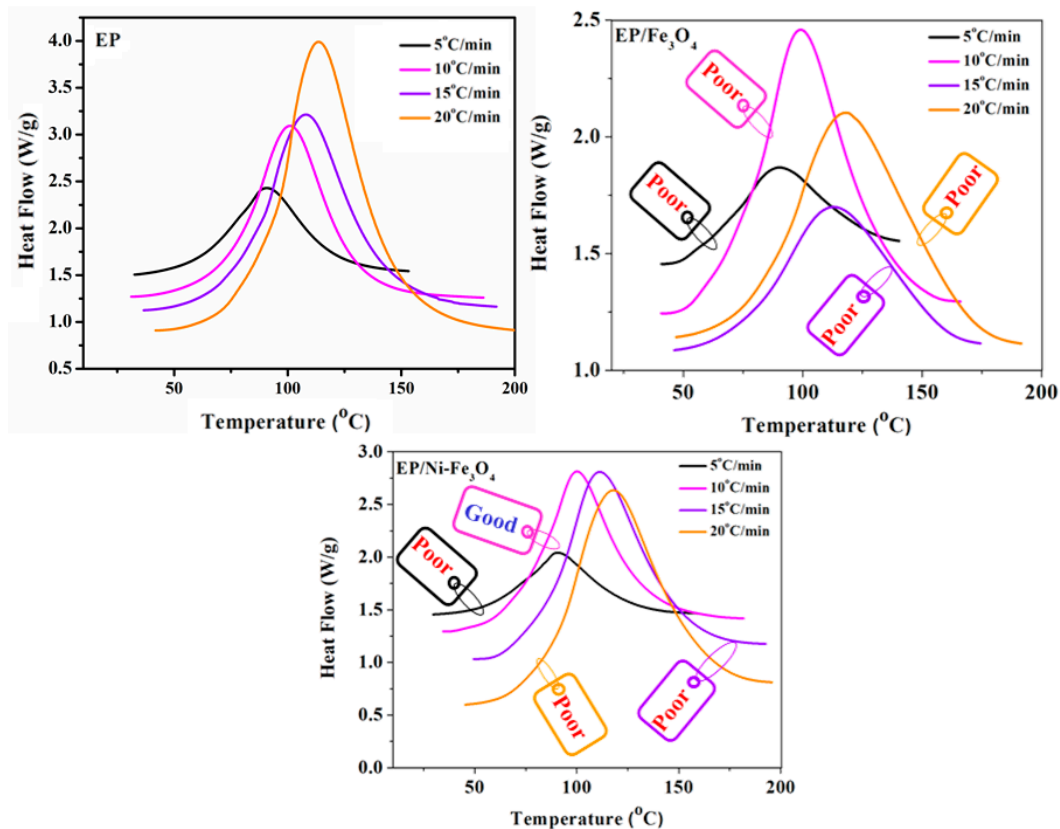


Figure 2. DSC profiles of epoxy (EP), EP/Fe₃O₄ and EP/Ni-Fe₃O₄ [13] nanocomposites at heating rates of 5, 10, 15 and 20 °C/min, where epoxy (EP) and EP/Fe₃O₄ are used as the control or reference samples. The labels are representative of the quality of cure according to the Cure Index [26]. It can be seen that the heating rate plays a key role in determining the cure states of nanocomposites.

When the vitrification takes place, the free volume between growing chains is reduced ending in a substantial drop in curing rate. Nevertheless, the vitrification phenomena gradually progress until a point where the cure temperature reaches the T_g . The mechanism at such conditions completely changes from chemical control to diffusion control.

The T_g of the fully cured neat epoxy and its nanocomposites containing 0.1 wt % of Fe₃O₄ and Ni-Fe₃O₄ at $\beta = 10$ °C/min reported in Table 1.

Table 1. T_g of the fully cured neat epoxy and its nanocomposites at β of 10 °C/min.

Sample	T_g (°C)
EP	100.2
EP/Fe ₃ O ₄	92.6
EP/Ni-Fe ₃ O ₄	101.5

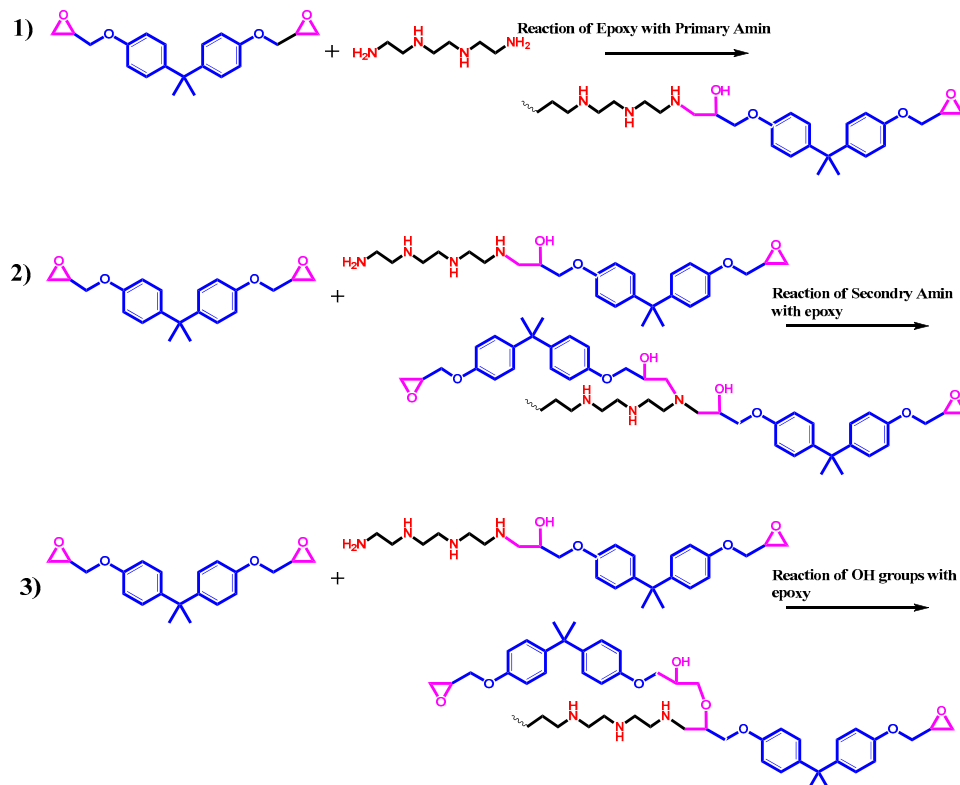


Figure 3. The typical reaction of epoxy with an amine-based curing agent.

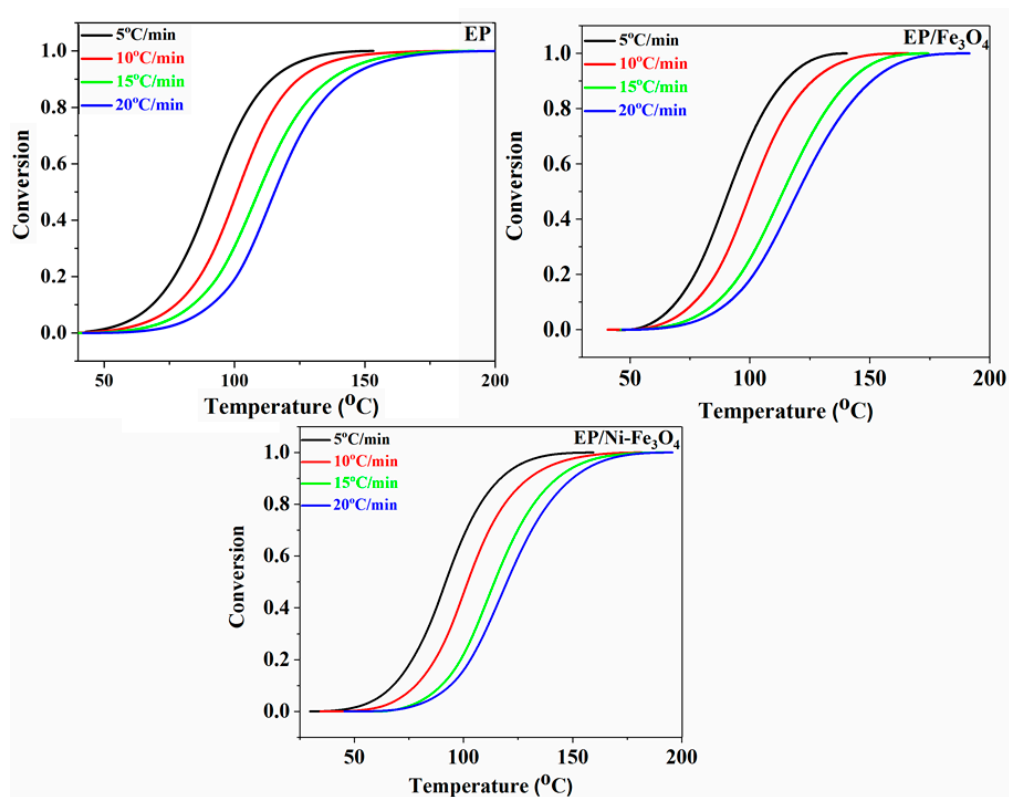


Figure 4. Profile variation of the fractional extent of cure, α versus reaction temperature for EP, EP/Fe₃O₄ [29] and EP/Ni-Fe₃O₄ nanocomposites at different heating rates of 5, 10, 15 and 20 °C/min. The sigmoidal shape of cures is an indication of the autocatalytic nature of crosslinking reactions independent of nanoparticle, and nanoparticle bulk and surface functionality.

The T_g of a thermoset epoxy directly depends on the segmental mobility of chains in the cured system [30]. In the EP/Fe₃O₄ system the reduction in the value of T_g from 100.2 °C for neat epoxy to 92.6 °C for the assigned composite indicates the weak interfacial interface between the epoxy resin and bare Fe₃O₄ nanoparticles. Accordingly, polymer chains can move easily in the vicinity of the Fe₃O₄ nanoparticles and epoxy resin because of the presence of free volume in this area. The reduction in the T_g of the EP/Fe₃O₄ system can be attributed to the hindrance of epoxy curing due to the reaction of Fe₃O₄ nanoparticles with the amine groups of hardeners. Therefore, the reactivity of amine groups of curing agents was decreased for reacting with epoxy resin. On the other hand, reactive Ni-doped MNPs can catalyze the epoxide ring-opening due to the Lewis acid effect of Ni²⁺ [31]. Therefore, the T_g of EP/Ni-Fe₃O₄ is slightly increased, suggesting confined molecular movements due to hindered segmental mobility of the polymer chains.

3.2. Cure Kinetics Analysis

Generally, a model-free approach also known as the isoconversional approach proposed for cure analysis is based on the monotonic dependence of the rate of curing reaction on temperature [32]. Model-free methods can successfully capture the variation of apparent activation energy ($E\alpha$) of cure reaction in terms of α [33]. The Friedman differential model [34] and the Flynn–Wall–Ozawa (FWO) and Kissinger–Akahira–Sunose (KAS) integral models are well-known isoconversional methods considered for determining $E\alpha$ [33]. In principle, the differential Friedman method should be more accurate than the KAS integral method because of no approximation being used, while the use of the Friedman method is associated with certain inaccuracies [33]. Although computationally not user-friendly, more accurate models are available for evaluating alteration of the $E\alpha$ of complex crosslinking reactions, especially in the initial and late stages of reaction [35]. Accordingly, both kinds of simple and practical differential Friedman and integral KAS isoconversional methods are routinely used in the analysis of nonisothermal kinetics. Moreover, due to the variety of approximations and mathematical formulation used in integral models, the results of activation energy by such methods may differ slightly from one to another, especially for KAS and FWO methods. Since in the FWO method the $E\alpha$ remains constant with the variation of α , the $E\alpha$ due to this model is used as the first trial in the determination of the kinetics model by the Malek method. The differential Friedman and integral KAS models and their fitting equation are mathematically and graphically explained in Section S1 of the supporting information (SI). Figure 5 is the main outcome of this part representing the variation of $E\alpha$ for EP, EP/Fe₃O₄ and EP/Ni-Fe₃O₄ nanocomposites with cure conversion in the curing reaction interval of $0.1 < \alpha < 0.9$ for differential Friedman and integral KAS models. Generally, the variation of $E\alpha$ with α over the whole reaction interval represents the complexity of the curing reaction. A slight decline in the $E\alpha$ value by increasing α in Figure 5, particularly for $\alpha > 0.3$, is due to the autocatalytic nature of the reaction of epoxy with an amine curing agent. Theoretically, the progress in crosslinking takes origin in the possibility of a chemical reaction between curing moieties prior to gelation in thermosetting systems. When viscosity increases due to the intensified crosslinking, a change in the state of curing of the chemical- to diffusion-controlled mechanism is likely to happen [36]. The gel point at which stepwise polymerization goes forward is dependent on the functionality of curing moieties. For an ideal reaction, an f -functional resin with a g -functional curing agent mixed in stoichiometric amounts can theoretically become gel at a theoretical point [37]:

$$x_{gel} = [(f - 1)(g - 1)]^{-1/2}, \quad (2)$$

For DGEBA epoxy resin ($f = 2$) with TETA curing agent ($g = 6$), the ideal gel conversion (x_{gel}) takes the value of ca. 0.45. Having this in mind, a drop in the value of the $E\alpha$ for $\alpha > 0.3$ could be due to the inaccuracy of the used isoconversional models or facilitated/accelerated autocatalytic ring-opening fueled by the hydroxyl functional groups generated in the early stage of reaction that activated in the middle stage. For nanocomposite samples, the presence of bare Fe₃O₄ nanoparticles hardens network

formation in the epoxy with respect to the blank epoxy, which increases the amount of energy needed for the species interacting with each other. However, the viscose system formed in the meanwhile acts in an opposite way to decline the E_a due to the incomplete curing caused by middle-state gelation. Fe_3O_4 nanoparticles in the epoxy/amine system have a higher tendency to react with more reactive amine groups of curing agents compared to epoxide rings which perturbs the stoichiometry of resin and hardener that leading to a decline in the apparent value of the E_a .

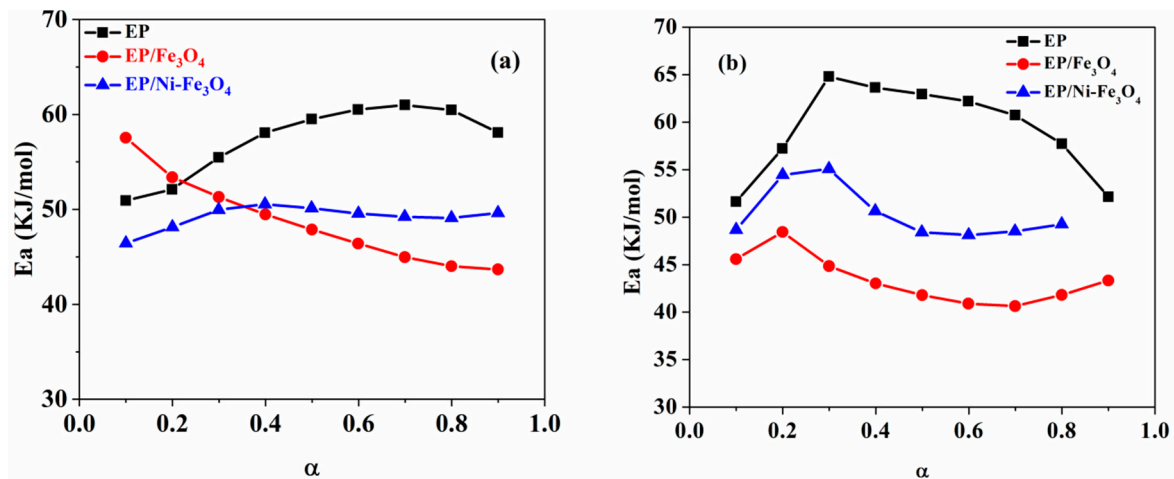


Figure 5. Variation of activation energy with conversion for EP, EP- Fe_3O_4 [22,29] and EP-Ni/ Fe_3O_4 nanocomposites estimated by the (a) differential Friedman model and (b) integral Kissinger–Akahira–Sunose (KAS) model.

For Ni- Fe_3O_4 , the doping stability of Ni decreases from the surface to the interior layers of the Fe_3O_4 lattice [38]. Therefore, it can be speculated that Ni dopants tended to locate on the top surface of lattice [39]. Ni-doping of Fe_3O_4 assisted in the formation of single nonagglomerated particles, which reflected in lower remanence magnetization (M_r) values for Ni- Fe_3O_4 (0.21 emu/g) compared to that of undoped Fe_3O_4 (0.95 emu/g) observed in VSM data. This indicates single domain centers formed in Ni- Fe_3O_4 contributed to the epoxy crosslinking reaction more efficiently compared with the undoped Fe_3O_4 . In addition, Ni^{2+} cations on the top layer of Fe_3O_4 crystal can act as Lewis acid sites and catalyze the ring-opening reaction between epoxy and amine curing agent [40,41]. Ni- Fe_3O_4 nanoparticles could participate in epoxide ring-opening through the reaction of -OH groups on the nanoparticle surface with oxirane rings and Ni^{2+} cations as Lewis acid sites. Ni- Fe_3O_4 nanoparticles have a more efficient role in curing reaction of epoxy compared to the Fe_3O_4 . Nevertheless, it was also likely that the reaction of Ni- Fe_3O_4 nanoparticles with amine groups of curing agents disturbed the stoichiometric balance between the epoxy prepolymer and amine curing agent as schematically shown in Figure 6. Therefore, EP/Ni- Fe_3O_4 nanocomposite also uses more energy for curing reaction compared to the EP/ Fe_3O_4 system leading to lower E_a value compared with that of neat epoxy.

Determining the Reaction Model and the Order of Reaction

The determination of the reaction model is of prime priority in monitoring the effect of Fe_3O_4 and Ni- Fe_3O_4 nanoparticles on the curing mechanism of the epoxy/amine system. For this purpose, the Friedman and Malek methods were used to assess whether the curing mechanism was autocatalytic or noncatalytic. Some important notes and mathematical relations in this regard can be found in Section S2 of SI. In the Friedman method, the curing mechanism can be proposed based on the shape of the plot of $\ln[Af(\alpha)]$ against $\ln(1 - \alpha)$ (Equation (S3)) showing a peak for α values between 0.2 and 0.4. Thus, the predicted reaction mechanism of the neat epoxy and its nanocomposites is autocatalytic.

The kinetic model should be determined before taking the next steps, which was done based on the Malek method using maximum points of $y(\alpha) = (\alpha_m)$, $z(\alpha) = (\alpha_p^\infty)$ and the peak conversion in the

DSC curves (α_p). The details of the Malek method are described in Section S2 of SI. The values of α_m , α_p and α_p^∞ for the prepared epoxy systems at different heating rates are reported in Table 2.

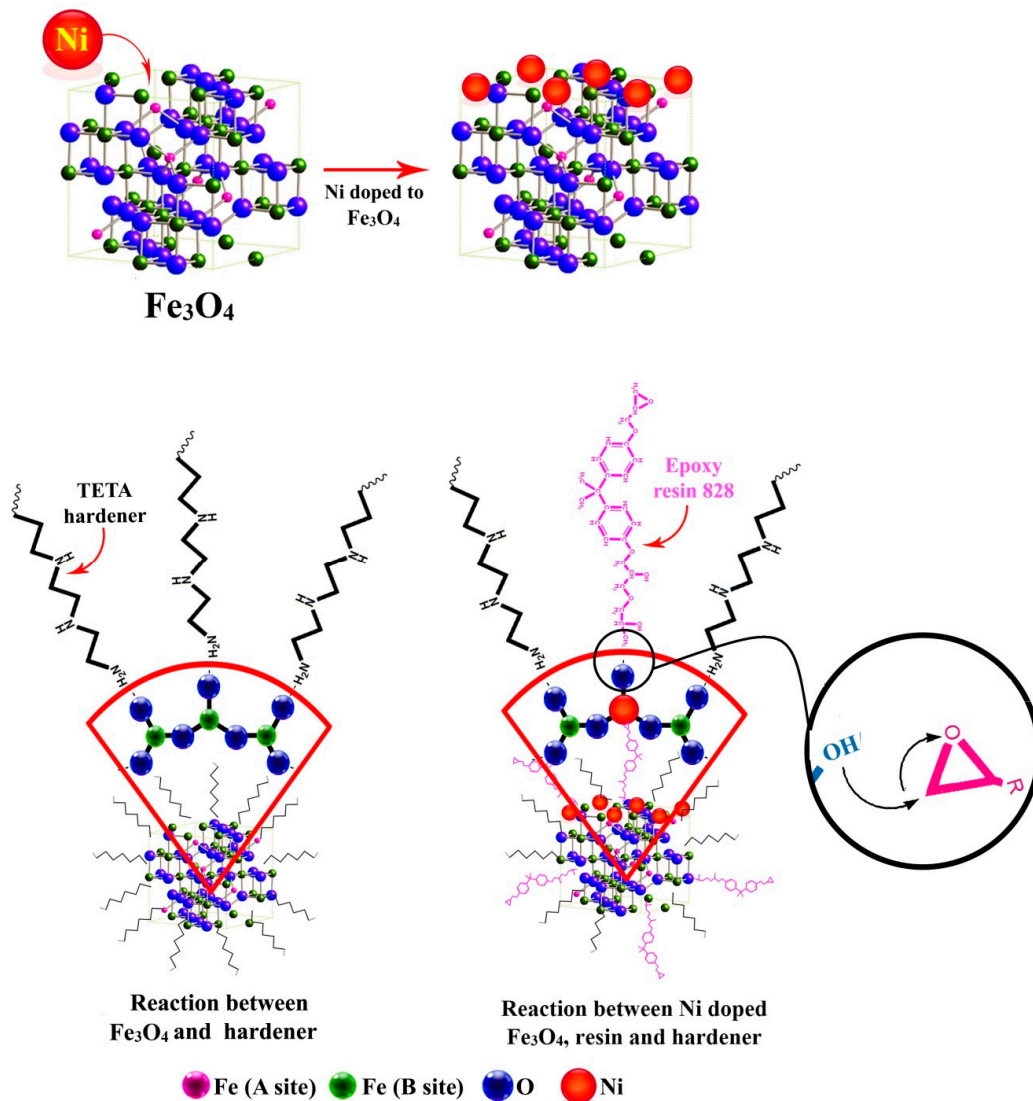


Figure 6. The possible reaction of Fe₃O₄ and Ni-Fe₃O₄ with the epoxy resin and the curing agent.

Table 2. The values of α_p , α_m and α_p^∞ obtained from the Malek model at various heating rates.

Designation	Heating Rate (°C/min)	α_p^∞	α_m	α_p
EP [22,29]	5	0.487	0.144	0.512
	10	0.555	0.073	0.510
	15	0.418	0.236	0.498
	20	0.383	0.251	0.483
EP/Fe ₃ O ₄ [22,29]	5	0.479	0.248	0.490
	10	0.407	0.279	0.491
	15	0.532	0.193	0.518
	20	0.462	0.201	0.491
EP/Ni-Fe ₃ O ₄	5	0.473	0.146	0.490
	10	0.400	0.296	0.475
	15	0.361	0.249	0.463
	20	0.514	0.208	0.487

According to Table 2, $\alpha_m < \alpha_p$ and at the same time $\alpha_p^\infty < 0.632$, suggesting that the two-parameter autocatalytic kinetic model should be considered for EP, EP/Fe₃O₄ and EP/Ni-Fe₃O₄.

As proved by Friedman and Malek models, the cure mechanism of EP, EP/Fe₃O₄ or EP/Ni-Fe₃O₄ nanocomposite is autocatalytic, which is defined by the following equation:

$$\frac{d\alpha}{dt} = A \exp\left(-\frac{E_\alpha}{RT}\right) \alpha^m (1 - \alpha)^n, \tag{3}$$

where n and m are the degrees of autocatalytic and noncatalytic reactions, and A is the pre-exponential factor. The values of triplet parameters (m , n and $\ln A$) were calculated from Equations (S11) and (S12) in Section S3 of SI. The E_α value was the average of the values obtained from the Friedman and KAS methods (Table 3).

Table 3. Parameters of cure kinetics obtained from the Friedman and KAS models as a function of heating rate.

Designation	Heating Rate (°C/min)	Friedman			KAS		
		m	n	$\ln A$ (s ⁻¹)	m	n	$\ln A$ (s ⁻¹)
EP [22,29]	5	0.41	1.54	18.80	0.43	1.52	18.18
	10	0.52	1.59	19.05	0.51	1.59	19.13
	15	0.44	1.68	18.98	0.46	1.66	18.39
	20	0.55	1.73	19.12	0.57	1.71	18.54
EP/Fe ₃ O ₄ [22,29]	5	0.36	1.22	13.25	0.30	1.27	15.01
	10	0.51	1.40	13.79	0.46	1.45	15.51
	15	0.32	1.18	13.24	0.25	1.23	14.89
	20	0.33	1.27	13.32	0.27	1.32	14.95
Epoxy/Ni-Fe ₃ O ₄	5	0.43	1.48	15.78	0.44	1.47	15.35
	10	0.55	1.68	16.24	0.57	1.66	15.82
	15	0.46	1.54	15.90	0.47	1.53	15.50
	20	0.41	1.51	15.83	0.43	1.49	15.43

As can be observed from Table 3, the triplet of kinetic parameters (n , m and $\ln A$) were obtained from both differential and integral methods. For EP, EP/Fe₃O₄ as well as EP/Ni-Fe₃O₄ nanocomposites, the overall order of crosslinking reaction ($m + n$) is higher than one, regardless of the heating rate, which is characteristic of the complexity of the curing reaction. The results in Table 3 suggest that by the addition of Fe₃O₄ nanoparticles a drop in the autocatalytic reaction order (m) is observed. This suggests a change in the curing trend from autocatalytic to noncatalytic, a signature of the nonreactive nature of Fe₃O₄ discussed earlier. By contrast, incorporation of Ni-Fe₃O₄ nanoparticles into the epoxy upsets the balance towards autocatalytic reaction, which was proved by an increase in the values of m compared to the EP/Fe₃O₄. Moreover, incorporation of Fe₃O₄ or Ni-Fe₃O₄ was the reason for reduced collisions in the systems between the cure moieties, which was detected by a reduction in the pre-exponential factor. Such findings approve the higher reactivity of Ni-Fe₃O₄ compared to Fe₃O₄, which means that doping in Ni facilitated epoxy ring-opening reactions due to the Lewis acid effect of Ni²⁺.

According to Equation (3), the curing reaction of epoxy with the hydrogen of primary amine at an early stage of the curing reaction can be explained by the kinetic exponent (n). The subsequent reaction comprises epoxy ring-opening reaction with the secondary amine and an autocatalytic ring-opening with a hydroxyl functional group formed in situ, which was tracked by a change in the kinetic exponent (m). At the low conversion of the curing reaction of epoxy resin, the crosslinking process is chemically controlled. On the other hand, in the vitrification stage (high values of α) diffusion dominates where the free volume of the crosslinked network decreases and the reaction will probably progress at a slower speed [42]. The diffusion effect in the epoxy system increases by progressing in the curing reaction from the onset of reaction up to vitrification. At the beginning of the reaction (low values of α), where the reaction is chemically controlled, condensation of monomers and oligomers is dominating,

therefore, diffusion can be overlooked. On the other hand, in the vitrification stage (high values of α) an infinite network is formed with very limited free-volumes in the crosslinked network; hence, the reaction probably happens at a slower speed [43]. The curing reaction of epoxy was expedited at higher conversions, where autocatalytic ring-opening was aided by the heat. According to Equation (3), the autocatalytic reaction exponent of m was changed to higher values. The observed fall in the m and $\ln A$ of epoxy nanocomposites compared to the neat epoxy (Table 3) revealed the difficulty in network formation with the autocatalytic reaction. It can be concluded that the vitrification in such a system prevented crosslinking to some extent.

The validation of the kinetic models based on the curing rate ($d\alpha/dt$) was calculated by determining $f(\alpha)$ and a comparison between the experimental and predicted values (Section S4 of SI). The curves calculated by Friedman and KAS methods using Equation (2) and the experimental curves for EP, EP/Fe₃O₄ and EP/Ni-Fe₃O₄ are shown in Figure S8, where the $d\alpha/dt$ values as the rate of cure reactions obtained theoretically by the isoconversional models are in confidence with the experimental values.

4. Conclusions

The triplet of cure parameters (n , m and $\ln A$) was obtained for epoxy nanocomposites containing Fe₃O₄ and Ni-Fe₃O₄ nanoparticles by modeling the cure kinetics. As a single peak was observed in DSC thermograms of all the prepared samples, it was concluded that a single step curing mechanism of the epoxy/amine system remained untouched with the introduction of Fe₃O₄ and Ni-Fe₃O₄ into the system. However, network formation was affected by the presence of nanoparticles. The variation of activation energy detected by isoconversional models (Friedman and KAS) unraveled hindered cure by the incorporation of the bare Fe₃O₄ nanoparticles due to the perturbation of stoichiometry between epoxy and curing agent because of the reaction of amine groups of hardeners with Fe₃O₄ nanoparticles. Accordingly, the activation energy of EP/Fe₃O₄ nanocomposite decreased due to the presence of less amount of amine curing agent compared to epoxy rings. On the other hand, doping Fe₃O₄ with Ni made the surface of nanoparticles reactive towards epoxy which arises from the Lewis acid effect of Ni²⁺ cations in catalyzing ring-opening reactions. Therefore, the activation energy of EP/Ni-Fe₃O₄ nanocomposite increased compared to EP/Fe₃O₄ nanocomposite due to the excessive reaction in the epoxy/amine system in the presence of Ni-Fe₃O₄ nanoparticles.

Supplementary Materials: The following are available online at <http://www.mdpi.com/2504-477X/4/3/102/s1>.

Author Contributions: Conceptualization, M.R.S.; methodology, S.M.R.P.; software, M.J. and Z.K.; validation, B.B. and P.Z.; formal analysis, M.J. and A.H.M.; investigation, M.R.G.; resources, P.V.P.; data curation, S.M.R.P.; writing—original draft preparation, M.J.; writing—review and editing, S.H.; visualization, M.R.S.; supervision, M.R.S. All authors have read and agreed to the published version of the manuscript.

Funding: This research received no external funding.

Conflicts of Interest: The authors declare no conflicts of interest. The funders had no role in the design of the study; in the collection, analyses, or interpretation of data; in the writing of the manuscript, or in the decision to publish the results.

References

1. Jouyandeh, M.; Tikhani, F.; Hampp, N.; Akbarzadeh Yazdi, D.; Zarrintaj, P.; Reza Ganjali, M.; Reza Saeb, M. Highly curable self-healing vitrimer-like cellulose-modified halloysite nanotube/epoxy nanocomposite coatings. *Chem. Eng. J.* **2020**, *396*, 125196. [[CrossRef](#)]
2. Jouyandeh, M.; Tikhani, F.; Shabaniyan, M.; Movahedi, F.; Moghari, S.; Akbari, V.; Gabrion, X.; Laheurte, P.; Vahabi, H.; Saeb, M.R. Synthesis, characterization, and high potential of 3D metal–organic framework (MOF) nanoparticles for curing with epoxy. *J. Alloys Compd.* **2020**, *829*, 154547. [[CrossRef](#)]
3. Jouyandeh, M.; Jazani, O.M.; Navarchian, A.H.; Saeb, M.R. Epoxy Coatings Physically Cured with Hydroxyl-contained Silica Nanospheres and Halloysite nanotubes. *Prog. Color Colorants Coat.* **2018**, *11*, 199–207.

4. Vryonis, O.; Virtanen, S.; Andritsch, T.; Vaughan, A.; Lewin, P. Understanding the cross-linking reactions in highly oxidized graphene/epoxy nanocomposite systems. *J. Mater. Sci.* **2019**, *54*, 3035–3051. [[CrossRef](#)]
5. Throckmorton, J.A.; Watters, A.L.; Geng, X.; Palmese, G.R. Room temperature ionic liquids for epoxy nanocomposite synthesis: Direct dispersion and cure. *Compos. Sci. Technol.* **2013**, *86*, 38–44. [[CrossRef](#)]
6. Mirabedini, S.; Behzadnasab, M.; Kabiri, K. Effect of various combinations of zirconia and organoclay nanoparticles on mechanical and thermal properties of an epoxy nanocomposite coating. *Compos. Part A Appl. Sci. Manuf.* **2012**, *43*, 2095–2106. [[CrossRef](#)]
7. Martin-Gallego, M.; Yuste-Sanchez, V.; Sanchez-Hidalgo, R.; Verdejo, R.; Lopez-Manchado, M.A. Epoxy nanocomposites filled with carbon nanoparticles. *Chem. Rec.* **2018**, *18*, 928–939. [[CrossRef](#)]
8. Samad, U.A.; Alam, M.A.; Chafidz, A.; Al-Zahrani, S.M.; Alharthi, N.H. Enhancing mechanical properties of epoxy/polyaniline coating with addition of ZnO nanoparticles: Nanoindentation characterization. *Prog. Org. Coat.* **2018**, *119*, 109–115. [[CrossRef](#)]
9. Cho, J.D.; Ju, H.T.; Park, Y.S.; Hong, J.W. Kinetics of Cationic Photopolymerizations of UV-curable epoxy-based SU8-negative photoresists with and without silica nanoparticles. *Macromol. Mater. Eng.* **2006**, *291*, 1155–1163. [[CrossRef](#)]
10. Ma, I.W.; Sh, A.; Ramesh, K.; Vengadaesvaran, B.; Ramesh, S.; Arof, A.K. Anticorrosion properties of epoxy-nanochitosan nanocomposite coating. *Prog. Org. Coat.* **2017**, *113*, 74–81.
11. Shi, X.; Nguyen, T.A.; Suo, Z.; Liu, Y.; Avci, R. Effect of nanoparticles on the anticorrosion and mechanical properties of epoxy coating. *Surf. Coat. Technol.* **2009**, *204*, 237–245. [[CrossRef](#)]
12. Madhup, M.K.; Shah, N.K.; Parekh, N.R. Investigation and improvement of abrasion resistance, water vapor barrier and anticorrosion properties of mixed clay epoxy nanocomposite coating. *Prog. Org. Coat.* **2017**, *102*, 186–193. [[CrossRef](#)]
13. Jouyandeh, M.; Paran, S.M.R.; Jannesari, A.; Saeb, M.R. 'Cure Index' for thermoset composites. *Prog. Org. Coat.* **2019**, *127*, 429–434. [[CrossRef](#)]
14. Tikhani, F.; Jouyandeh, M.; Jafari, S.H.; Chabokrow, S.; Ghahari, M.; Gharanjig, K.; Klein, F.; Hampp, N.; Ganjali, M.R.; Formela, K. Cure Index demonstrates curing of epoxy composites containing silica nanoparticles of variable morphology and porosity. *Prog. Org. Coat.* **2019**, *135*, 176–184. [[CrossRef](#)]
15. Jouyandeh, M.; Ganjali, M.R.; Ali, J.A.; Aghazadeh, M.; Karimzadeh, I.; Formela, K.; Colom, X.; Cañavate, J.; Saeb, M.R. Curing epoxy with ethylenediaminetetraacetic acid (EDTA) surface-functionalized $\text{CoFe}_{3-x}\text{O}_4$ magnetic nanoparticles. *Prog. Org. Coat.* **2019**, 105248. [[CrossRef](#)]
16. Jouyandeh, M.; Zarrintaj, P.; Ganjali, M.R.; Ali, J.A.; Karimzadeh, I.; Aghazadeh, M.; Ghaffari, M.; Saeb, M.R. Curing epoxy with electrochemically synthesized $\text{GdFe}_{3-x}\text{O}_4$ magnetic nanoparticles. *Prog. Org. Coat.* **2019**, 105245. [[CrossRef](#)]
17. Jouyandeh, M.; Ganjali, M.R.; Ali, J.A.; Aghazadeh, M.; Paran, S.M.R.; Naderi, G.; Saeb, M.R.; Thomas, S. Curing epoxy with polyvinylpyrrolidone (PVP) surface-functionalized $\text{ZnFe}_{3-x}\text{O}_4$ magnetic nanoparticles. *Prog. Org. Coat.* **2019**, 105227. [[CrossRef](#)]
18. Jouyandeh, M.; Paran, S.M.R.; Jannesari, A.; Puglia, D.; Saeb, M.R. Protocol for nonisothermal cure analysis of thermoset composites. *Prog. Org. Coat.* **2019**, *131*, 333–339. [[CrossRef](#)]
19. Jouyandeh, M.; Shabaniyan, M.; Khaleghi, M.; Paran, S.M.R.; Ghiyasi, S.; Vahabi, H.; Formela, K.; Puglia, D.; Saeb, M.R. Acid-aided epoxy-amine curing reaction as reflected in epoxy/ Fe_3O_4 nanocomposites: Chemistry, mechanism, and fracture behavior. *Prog. Org. Coat.* **2018**, *125*, 384–392. [[CrossRef](#)]
20. Jouyandeh, M.; Paran, S.M.R.; Shabaniyan, M.; Ghiyasi, S.; Vahabi, H.; Badawi, M.; Formela, K.; Puglia, D.; Saeb, M.R. Curing behavior of epoxy/ Fe_3O_4 nanocomposites: A comparison between the effects of bare Fe_3O_4 , $\text{Fe}_3\text{O}_4/\text{SiO}_2/\text{chitosan}$ and $\text{Fe}_3\text{O}_4/\text{SiO}_2/\text{chitosan/imide/phenylalanine}$ -modified nanofillers. *Prog. Org. Coat.* **2018**, *123*, 10–19. [[CrossRef](#)]
21. Jouyandeh, M.; Ganjali, M.R.; Ali, J.A.; Aghazadeh, M.; Stadler, F.J.; Saeb, M.R. Curing epoxy with electrochemically synthesized $\text{Ni}_x\text{Fe}_{3-x}\text{O}_4$ magnetic nanoparticles. *Prog. Org. Coat.* **2019**, 105198. [[CrossRef](#)]
22. Jouyandeh, M.; Karami, Z.; Hamad, S.M.; Ganjali, M.R.; Akbari, V.; Vahabi, H.; Kim, S.-J.; Zarrintaj, P.; Saeb, M.R. Nonisothermal cure kinetics of epoxy/ $\text{ZnFe}_{3-x}\text{O}_4$ nanocomposites. *Prog. Org. Coat.* **2019**, *136*, 105290. [[CrossRef](#)]
23. Karami, Z.; Jouyandeh, M.; Ali, J.A.; Ganjali, M.R.; Aghazadeh, M.; Paran, S.M.R.; Naderi, G.; Puglia, D.; Saeb, M.R. Epoxy/layered double hydroxide (LDH) nanocomposites: Synthesis, characterization, and Excellent cure feature of nitrate anion intercalated Zn-Al LDH. *Prog. Org. Coat.* **2019**, *136*, 105218. [[CrossRef](#)]

24. Jouyandeh, M.; Ali, J.A.; Akbari, V.; Aghazadeh, M.; Paran, S.M.R.; Naderi, G.; Saeb, M.R.; Ranjbar, Z.; Ganjali, M.R. Curing epoxy with polyvinylpyrrolidone (PVP) surface-functionalized $\text{MnxFe}_{3-x}\text{O}_4$ magnetic nanoparticles. *Prog. Org. Coat.* **2019**, 105247. [[CrossRef](#)]
25. Jouyandeh, M.; Ganjali, M.R.; Ali, J.A.; Aghazadeh, M.; Saeb, M.R.; Ray, S.S. Curing epoxy with polyvinylpyrrolidone (PVP) surface-functionalized $\text{NixFe}_{3-x}\text{O}_4$ magnetic nanoparticles. *Prog. Org. Coat.* **2019**, 105259. [[CrossRef](#)]
26. Jouyandeh, M.; Jazani, O.M.; Navarchian, A.H.; Shabaniyan, M.; Vahabi, H.; Saeb, M.R. Surface engineering of nanoparticles with macromolecules for epoxy curing: Development of super-reactive nitrogen-rich nanosilica through surface chemistry manipulation. *Appl. Surf. Sci.* **2018**, 447, 152–164. [[CrossRef](#)]
27. Lange, J.; Altmann, N.; Kelly, C.; Halley, P. Understanding vitrification during cure of epoxy resins using dynamic scanning calorimetry and rheological techniques. *Polymer* **2000**, 41, 5949–5955. [[CrossRef](#)]
28. Bayat, S.; Moini Jazani, O.; Molla-Abbasi, P.; Jouyandeh, M.; Saeb, M.R. Thin films of epoxy adhesives containing recycled polymers and graphene oxide nanoflakes for metal/polymer composite interface. *Prog. Org. Coat.* **2019**, 136, 105201. [[CrossRef](#)]
29. Jouyandeh, M.; Paran, S.M.R.; Khadem, S.S.M.; Ganjali, M.R.; Akbari, V.; Vahabi, H.; Saeb, M.R. Nonisothermal cure kinetics of epoxy/ $\text{MnxFe}_{3-x}\text{O}_4$ nanocomposites. *Prog. Org. Coat.* **2020**, 140, 105505. [[CrossRef](#)]
30. Jouyandeh, M.; Jazani, O.M.; Navarchian, A.H.; Shabaniyan, M.; Vahabi, H.; Saeb, M.R. Bushy-surface hybrid nanoparticles for developing epoxy superadhesives. *Appl. Surf. Sci.* **2019**, 479, 1148–1160. [[CrossRef](#)]
31. Otto, S.; Engberts, J.B. Lewis-acid catalysis of a Diels-Alder reaction in water. *Tetrahedron Lett.* **1995**, 36, 2645–2648. [[CrossRef](#)]
32. Wan, J.; Li, C.; Bu, Z.-Y.; Xu, C.-J.; Li, B.-G.; Fan, H. A comparative study of epoxy resin cured with a linear diamine and a branched polyamine. *Chem. Eng. J.* **2012**, 188, 160–172. [[CrossRef](#)]
33. Vyazovkin, S.; Burnham, A.K.; Criado, J.M.; Pérez-Maqueda, L.A.; Popescu, C.; Sbirrazzuoli, N. ICTAC Kinetics Committee recommendations for performing kinetic computations on thermal analysis data. *Thermochim. Acta* **2011**, 520, 1–19. [[CrossRef](#)]
34. Miura, K. A New and Simple Method to Estimate $f(E)$ and $k_0(E)$ in the Distributed Activation Energy Model from Three Sets of Experimental Data. *Energy Fuels* **1995**, 9, 302–307. [[CrossRef](#)]
35. Vyazovkin, S. Model-free kinetics. *J. Therm. Anal. Calorim.* **2006**, 83, 45–51. [[CrossRef](#)]
36. Ratna, D. *Handbook of Thermoset Resins*; ISmithers: Shawbury, UK, 2009.
37. Pascault, J.-P.; Williams, R.J. *Epoxy Polymers: New Materials and Innovations*; John Wiley & Sons: Hoboken, NJ, USA, 2009.
38. Fu, Z.; Yang, B.; Zhang, Y.; Zhang, N.; Yang, Z. Dopant segregation and CO adsorption on doped Fe_3O_4 (1 1 1) surfaces: A first-principle study. *J. Catal.* **2018**, 364, 291–296. [[CrossRef](#)]
39. Reddy, G.K.; Gunasekera, K.; Boolchand, P.; Dong, J.; Smirniotis, P.G. High temperature water gas shift reaction over nanocrystalline copper codoped-modified ferrites. *J. Phys. Chem. C* **2011**, 115, 7586–7595. [[CrossRef](#)]
40. Sari, M.G.; Saeb, M.R.; Shabaniyan, M.; Khaleghi, M.; Vahabi, H.; Vagner, C.; Zarrintaj, P.; Khalili, R.; Paran, S.M.R.; Ramezanzadeh, B.; et al. Epoxy/starch-modified nano-zinc oxide transparent nanocomposite coatings: A showcase of superior curing behavior. *Prog. Org. Coat.* **2018**, 115, 143–150. [[CrossRef](#)]
41. Rastin, H.; Saeb, M.R.; Nonahal, M.; Shabaniyan, M.; Vahabi, H.; Formela, K.; Gabrion, X.; Seidi, F.; Zarrintaj, P.; Sari, M.G.; et al. Transparent nanocomposite coatings based on epoxy and layered double hydroxide: Nonisothermal cure kinetics and viscoelastic behavior assessments. *Prog. Org. Coat.* **2017**, 113, 126–135. [[CrossRef](#)]
42. Zhao, K.; Wang, J.; Song, X.; Liang, C.; Xu, S. Curing kinetics of nanostructured epoxy blends toughened with epoxidized carboxyl-terminated liquid rubber. *Thermochim. Acta* **2015**, 605, 8–15. [[CrossRef](#)]
43. Huguenin, F.G.; Klein, M.T. Intrinsic and transport-limited epoxyamine cure kinetics. *Ind. Eng. Chem. Prod. Res. Dev.* **1985**, 24, 166–171. [[CrossRef](#)]

